LINC01635, a long non-coding RNA with a cancer/testis expression pattern, promotes lung cancer progression by sponging miR-455-5p

WENYI SHEN[1*], JUAN PU[2*], SHANYE GU[3], JING SUN[1], LILI WANG[1], BIN TAN[1], JIANMENG CHEN[1] and YANGSONG ZUO[1]

[1]Department of Respiratory Medicine, [2]Department of Radiotherapy and [3]Clinical Laboratory, Lianshui County People's Hospital, Kangda College of Nanjing Medical University, Huai'an, Jiangsu 223400, P.R. China

Received February 14, 2022; Accepted September 12, 2022

DOI: 10.3892/ol.2022.13558

Abstract. Long non-coding RNAs (lncRNAs) have been reported to play vital roles in human lung cancer. In recent years, cancer/testis (CT) lncRNAs have been characterized as a novel class of lncRNA. However, this class of lncRNA remains to be thoroughly investigated. The present study identified long intergenic non-protein coding RNA 1635 (LINC01635), which was highly expressed in testis and in a broad range of human cancer types. Next, it was confirmed that LINC01635 was upregulated significantly in samples from patients with lung cancer and in non-small cell lung carcinoma (NSCLC) cell lines. Silencing LINC01635 suppressed the proliferation and metastasis of NSCLC cells *in vitro* and *in vivo*. Furthermore, it was found that LINC01635 could bind to microRNA (miRNA or miR)-455-5p and regulate the expression of a series of miR-455-5p-targeting tumor-related genes. Knockdown of miR-455-5p partially rescued the progression of lung cancer cells that was suppressed by LINC01635 silencing. Together, the current results demonstrated that LINC01635 may play important roles in NSCLC progression by targeting miR-455-5p, and that it could be a biomarker and therapeutic target for lung cancer.

Introduction

Lung cancer is one of the most malignant tumors and is the leading cause of cancer-associated mortality worldwide (1,2). Among patients with lung cancer, non-small cell lung carcinoma (NSCLC) accounts for ~85% of all cases (3,4). Despite the development of novel therapies in the past few decades, the 5-year survival rate (4-17% depending on stage and regional differences) of patients with NSCLC remains markedly low (5); this is due to the difficulty in early diagnosis, the lack of targeted therapies, drug resistance and frequent relapses. Therefore, identifying new biomarkers for early diagnosis and new therapies is essential for the clinical treatment of NSCLC.

Bioinformatics analysis of the human genome showed that <2% of the genome sequence corresponds to protein-coding genes, whereas >70% is transcribed into non-coding RNAs (ncRNAs) (6). Long ncRNAs (lncRNAs) are an important type of ncRNAs, with a length of >200 nucleotides. lncRNAs have been reported to play important roles in various tumor types, such as lung, colorectal and breast cancer, through multiple mechanisms (7,8). By comparative analysis of microarray and next-generation sequencing data of NSCLC and normal tissues, thousands of lncRNAs were identified to be differentially expressed in NSCLC samples (9-12). Although a few of studies have shown that several lncRNAs could promote or suppress the progression of NSCLC (13), identifying novel oncogenic lncRNAs remains critical for NSCLC diagnosis and treatment.

Cancer/testis (CT) antigens are the protein products of genes frequently expressed in multiple human cancer types and in the normal testis (14,15). To date, only a few lncRNAs have been reported to be CT genes (16-19). The present study identified long intergenic non-protein coding RNA 1635 (LINC01635) as a potential novel CT lncRNA. The expression of LINC01635 in lung cancer was investigated, and it was found that LINC01635 was highly expressed in samples from patients with lung cancer and in NSCLC cell lines. Functional studies showed that LINC01635 regulated the proliferation and metastasis of NSCLC cells *in vitro* and *in vivo*. Furthermore, it was also found that LINC01635 could bind to microRNA (miRNA/miR)-455-5p *in vitro* and that it regulated the expression of miR-455-5p-targeting tumor-related genes in NSCLC cells, which demonstrated its functional mechanism in lung cancer.

Correspondence to: Dr Yangsong Zuo, Department of Respiratory Medicine, Lianshui County People's Hospital, Kangda College of Nanjing Medical University, 6 Hongri Avenue, Huai'an, Jiangsu 223400, P.R. China
E-mail: zys126@njmu.edu.cn

*Contributed equally

Key words: long non-coding RNA, cancer/testis long non-coding RNAs, long intergenic non-protein coding RNA 1635, microRNA-455-5p, non-small cell lung carcinoma

Materials and methods

lncRNA selection with CT expression pattern from lung cancer RNA-expression data. Microarray dataset GSE113852 (20) was downloaded from the Gene Expression Omnibus (GEO) database (https://www.ncbi.nlm.nih.gov/geo/), and LINC01635 expression profiling in normal tissue was analyzed according to the data of the RNA-sequencing (RNA-seq) of normal tissues in the Human Protein Atlas (https://www.ncbi.nlm.nih.gov/). The coding potential of LINC01635 was assessed using the CPAT and CNCI online tools (https://lncar.renlab.org/), and the expression level of LINC01635 was also confirmed by analyzing another microarray dataset (GSE101929) (21) using online tools (https://lncar.renlab.org/) (22). LINC01635 expression profiling in different tumors and normal tissues was analyzed online by Gene Expression Profiling Interactive Analysis using RNA-seq data from The Cancer Genome Atlas (TCGA) and Genotype-Tissue Expression (GTEx) databases (http://gepia.cancer-pku.cn/) (23).

Clinical samples. A total of 14 paired human NSCLC and adjacent normal lung tissues were obtained from patients who underwent surgery or biopsy at Lianshui County People's Hospital, Kangda College of Nanjing Medical University (Lianshui, China) (mean age, 69 years; range, 50-80 years) between December 2018 and December 2019. All patients were diagnosed with NSCLC according to histopathological evaluation. No radiotherapy or chemotherapy was performed prior to sample collection. Tissue samples were immediately stored in RNAlater solution (Invitrogen; Thermo Fisher Scientific, Inc.) at -80˚C. Written informed consents was obtained from all the enrolled patients with NSCLC. The study protocol was approved by the Research Ethics Committee of Lianshui County People's Hospital, Kangda College of Nanjing Medical University (approval no. 2021602-2).

Cell culture. The human NSCLC A549, H1299, H1975 and PC9 cell lines, and the human bronchial epithelial HBE135-E6E7 cell line (HBE135) were obtained from the Institute of Biochemistry and Cell Biology of Chinese Academy of Sciences. A549, H1975 and HBE135 cells were cultured in RPMI-1640 medium (Gibco; Thermo Fisher Scientific, Inc.), while H1299 and PC9 cells were cultured in DMEM (Gibco; Thermo Fisher Scientific, Inc.). Both media were supplemented with 10% fetal bovine serum (FBS; Gibco; Thermo Fisher Scientific, Inc.), 100 U/ml penicillin and 100 mg/ml streptomycin. All cell lines were maintained in a humidified air atmosphere with 5% CO_2 at 37˚C.

RNA extraction and reverse transcription-quantitative PCR (RT-qPCR). Total RNA was extracted from patient tissues and cultured cells using TRIzol® reagent (Ambion; Thermo Fisher Scientific, Inc.). A total of 1 μg of RNA was reversed transcribed to cDNA with the PrimeScript RT Reagent Kit (Takara Biotechnology Co., Ltd.) by using 6-mer random primers or a miR-455-5p specific primer (5'-GTTGGCTCT GGTGCAGGGTCCGAGGTATTCGCACCAGAGCCAACC GATGT-3') based on the stem-loop primer method (24). The reaction conditions were as follows: 42˚C for 2 min, 25˚C for 5 min, 42˚C for 30 min and 85˚C for 5 min. qPCR was then performed using SYBR-Green Master Mix (Takara Biotechnology Co., Ltd.) in a StepOnePlus™ Real-Time PCR System (Applied Biosystems; Thermo Fisher Scientific, Inc.) according to the manufacturer's instructions. The thermocycling conditions for qPCR were as follows: 95˚C for 5 min for 1 cycle, and 95˚C for 10 sec and 60˚C for 30 sec for 40 cycles. The endogenous control was GAPDH or U6 (for miR-455-5p), and the expression levels were analyzed by the $2^{-\Delta\Delta Cq}$ method (25). The specific primers were designed with Primer-Blast (National Center for Biotechnology; National Institutes of Health), and the primer sequences are listed in Table I. All primers were synthesized by General Biosystems, Inc.

Cloning of LINC01635. Primers were designed according to the prediction of LINC01635 transcripts in the Ensembl website (https://www.ensembl.org/) and the human mRNA clone of LINC01635 (GenBank ID: BC039533), and LINC01635 was cloned using the cDNA of A549 cell lines by ExTaq (Takara Biotechnology Co., Ltd.) in a Mastercycler® Nexus X2 (Eppendorf). The following thermocycling conditions were used: 94˚C for 5 min for 1 cycle, and 94˚C for 30 sec, 60˚C for 30 sec and 72˚C for 2 min for 35 cycles. The primer sequences were as follows: 5'-TTACCGTGCGGAGTT TTGGA-3' (forward) and 5'-TTATGTGCCTATGAAATT GGAGTTG-3' (reverse).

Small RNA transfection. LINC01635 small interfering (si)RNA (si-LINC01635), negative control (NC) siRNA, miR-455-5p inhibitor and NC inhibitor were purchased from General Biosystems and used for transiently down-regulating the expression of LINC01635 or miR-455-5p. The sequences of the synthesized siRNAs and miRNA inhibitors were as follows: 5'-GGAGUUUUGGAUACA UUCU-3' (si-LINC01635), 5'-UUCUCCGAACGUGUC ACGU-3' (NC siRNA), 5'-UAUGUGCCUUUGGACUAC AUCG-3' (miR-455-5p inhibitor) and 5'-UCUACUCUU UCUAGGAGGUUGUGA-3' (NC inhibitor). miR-455-5p mimic and NC miRNA mimic were also purchased from General Biosystems and used for transiently upregulating the expression of miR-455-5p. The sequences of the synthesized miRNA mimics were as follows: 5'-UAUGUGCCUUUG GACUACAUCG-3' (miR-455-5p mimic) and 5'-UCACAA CCUCCUAGAAAGAGUAGA-3' (NC mimic).

A549 and H1975 cells ($1x10^5$) were seeded in 6-well plates and cultured at 37˚C overnight. Next, the cells were transfected with siRNAs (50 μM), miRNA mimics (50 μM) or miRNA inhibitors (100 μM) for 24 h at 37˚C using Lipofectamine® 2000 reagent (Invitrogen; Thermo Fisher Scientific, Inc.) according to the manufacturer's instructions. At 24 h post-transfection, the knockdown efficiency was detected by RT-qPCR.

Cell proliferation assay. A cell proliferation assay was performed using Cell Counting Kit-8 (CCK-8; Dojindo Laboratories, Inc.). A549 and H1975 cells transfected with siRNA-LINC01635 and NC siRNA were seeded at $2x10^3$ cells/well in 96-well plates. Next, 10 μl CCK-8 reagent was added to each well, which contained 100 μl culture medium. After 2 h, cell proliferation was monitored by measuring the optical density at 450 nm on a microplate reader (BioTek Elx800;

Table I. Primer sequences for reverse transcription-quantitative PCR.

Molecule	Primer sequence (5'-3')
GAPDH-F	GGGAGCCAAAAGGGTCAT
GAPDH-R	GAGTCCTTCCACGATACCAA
LINC01635-F	GGGCCCCATTCTGAGGTTAC
LINC01635-R	GCGCCAATACAAGGACCACT
SOX11-F	GGTGGATAAGGATTTGGATTCG
SOX11-R	GCTCCGGCGTGCAGTAGT
RAB18-F	CAATGTGCCTTTGAAGAACTTGT
RAB18-R	CTCCTTGGCCTTCTTCCCTG
TMED2-F	ATGTATTCCTGTTCGTGCTT
TMED2-R	CACATGGATGGAACATACAA
USP3-F	AGGTGCTATGCTTACATTTG
USP3-R	CTGTTCTCAGGCTCTAGTAAG
CDKN1B-F	GCCGCAACCAATGGATCTCCTC
CDKN1B-R	AGTCGCAGAGCCGTGAGCAA
CPEB1-F	CACAGATAAGCACAAGTATC
CPEB1-R	GACACAGAGAATCTTCTAG
UBE2V1-F	AAAAGTCCCTCGCAATTTCC
UBE2V1-R	CTGCCATTTTGCTAGCACTG
HDAC4-F	AGAATGGCTTTGCTGTGGTC
HDAC4-R	ATCTTGCTCACGCTCAACCT
STK24-F	GCCTCCACCAAGATATTCCA
STK24-R	AACAAGAAATCACAGTGCTGAGTC
MMP2-F	CTGCGGTTTTCTCGAATCCATG
MMP2-R	GTCCTTACCGTCAAAGGGGTATCC
MMP9-F	GAGGCGCTCATGTACCCTATGTAC
MMP9-R	GTTCAGGGCGAGGACCATAGAG
LINC00339-F	TCTTTCCATTTTGCAGTTGGGC
LINC00339-R	CTCCTCGGCCCATCATTTCAT
U6-F	GCTTCGGCAGCACATATACTAAAAT
U6-R	CGCTTCACGAATTTGCGTGTCAT
miR-455-5p-F	GCCGCCTATGTGCCTTTGGACT
miR-455-5p-R	GTGCAGGGTCCGAGGT

F, forward; R, reverse; LINC01635, long intergenic non-protein coding RNA 1635; RAB18, ras-related protein Rab-18; TMED2, transmembrane P24 trafficking protein 2; USP3, ubiquitin specific peptidase 3; CDKN1B, cyclin-dependent kinase inhibitor 1B; CPEB1, cytoplasmic polyadenylation element binding protein 1; UBE2V1, ubiquitin conjugating enzyme E2 V1; HDAC4, histone deacetylase 4; STK24, serine/threonine kinase 24; LINC00339, long intergenic non-protein coding RNA 339; miR, microRNA.

BioTek Instruments, Inc.) every 24 h from 0 to 96 h according to the manufacturer's instructions.

Transwell assay. Cell migration was analyzed by Transwell assay. A549 and H1975 cells were transfected with si-LINC01635, NC siRNA, miR-455-5p inhibitor, NC inhibitor or siRNA + inhibitor, and then re-suspended with 200 μl serum-free medium to a total of 2-5x10^4 A549 cells or 5x10^4 H1975 cells. Transwell chambers (8-μm pore size) were placed into 24-well plates, and 800 μl medium containing 10% FBS was added to the lower chamber. After 24 h at 37˚C, the upper chambers were fixed with methanol for 30 min at room temperature, and then stained with 0.1% crystal violet for 20 min at room temperature. Next, the upper surface of the membrane was removed with cotton swabs. The Transwell inserts were imaged under an optical inverted microscope.

Western blotting. Total protein from transfected lung cancer cells was extracted with RIPA lysis buffer (Beyotime Institute of Biotechnology). The protein concentration was measured with a BCA kit (Beyotime Institute of Biotechnology). The protein samples (50 μg per lane) were separated on 10% gels using SDS-PAGE and then were electro-transferred onto polyvinylidene fluoride membranes (MilliporeSigma), which were blocked with 5% skimmed milk for 1 h at room temperature. Subsequently, the membranes were incubated with primary antibodies against MMP2 (1:1,000; cat. no. A00286), MMP9 (1:1,000; cat. no. PB0709) or GAPDH (internal control; 1:10,000; cat. no. A00227) (all Boster Biological Technology) at 4˚C overnight. Next, the membranes were incubated with HRP-conjugated AffiniPure mouse anti-rabbit IgG (H+L) (1:5,000; cat. no. BM2006; Boster Biological Technology) for 1 h at room temperature. After washing for 5 times (each for 5 min) using PBST (0.05% Tween-20) at room temperature, the proteins were visualized with the BeyoECL plus kit (Beyotime Institute of Biotechnology).

Zebrafish xenograft models. Zebrafish were maintained in a fish culture system (Haisheng Instruments, Inc.) at 28˚C under a light-dark cycle of 10-14 h. Approximately 100 2-days post-fertilization (dpf) transgenic Tg(fli1a:EGFP) zebrafish larvae (China Zebrafish Resource Center) were used for cell injection, and the endothelial cells of these transgenic zebrafish larvae were labeled with EGFP (26). At 24 h post-transfection of si-LINC01635 or NC siRNA (control) in cultured cells, including A549 and H1975 cell lines, the cells were collected and stained for 5 min at 37˚C and 15 min at 4˚C with a fluorescent dye (CM-DiI; Thermo Fisher Scientific, Inc.) for injection. The stained cells were examined under a fluorescence microscope before injection. A total of 300-400 cells labeled with CM-DiI were transplanted into the perivitelline space (PVS) of 48-h-post-fertilization zebrafish larvae under a pressure systems for ejection (Picosprizer III; Parker Hannifin Corporation). At 1 day post-injection (dpi), the injected larvae with similar tumor size of CM-DiI-positive cells were selected and cultured at 34˚C until the end of experiments. At 4 dpi, the intact zebrafish larvae were mounted using 1.2% low-melting gel, and the yolk and trunk were imaged via a stereomicroscope (MVX10; Olympus Corporation) or a confocal microscope (FLUOVIEW FV3000; Olympus Corporation) using a 20X water-immersion objective directly. The spatial resolution of the images was 1,600x1,200 pixels for the MVX10 or 1,024x1,024 pixels for the FLUOVIEW FV3000. After the imaging experiments, zebrafish larvae were anesthetized with alcohol and then sacrificed by hypothermia (-20˚C).

miRNA binding prediction. miRNAs that could potentially bind to LINC01635 were predicted by the online tools miRDB (http://mirdb.org/) and LncBase (http://www.microrna.gr/LncBase).

The miRNAs that were predicted by both tools were considered as candidates. miRNA-targeting genes were predicted by the online tools miRDB (http://mirdb.org/) and TargetScan (https://www.targetscan.org/). The tumor-related targeted genes of interest were screened out individually by scientific literature search using the key words 'tumor' and the name of each miRNA in PubMed (https://pubmed.ncbi.nlm.nih.gov/).

Isolation of cytoplasmic and nuclear RNA. A total of $1x10^7$ A549 cells were collected, and their cytoplasmic and nuclear RNA were extracted respectively with the PARIS™ Kit (Invitrogen; Thermo Fisher Scientific, Inc.) according to the manufacturer's instructions. Next, the cytoplasmic and nuclear RNA were reverse-transcribed, respectively. Then, the expression levels of cytoplasmic and nuclear RNA were detected by RT-qPCR, which represented the localization of RNA. U6 was used for the positive control of nuclear RNA, and GAPDH was used for the positive control of cytoplasmic RNA.

Reporter plasmid construction and luciferase reporter assay. The total sequence of LINC01635 transcript 1# was cloned into a pmirGLO Dual-Luciferase miRNA Target Expression Vector (E1330; Promega Corporation) to generate the reporter plasmid. To construct a LINC01635 mutant reporter plasmid, the putative binding site of miR-455-5p in LINC01635 was mutated by PCR.

The plasmids and miR-455-5p mimic or NC mimic were co-transfected into $2x10^4$ 293T cells (Saihongrui Biotechnology Co., Ltd.) cultured in DMEM with 10% FBS) at 37˚C for 48 h using Lipofectamine® 2000 reagent (Invitrogen; Thermo Fisher Scientific, Inc.) according to the manufacturer's instructions. The luciferase activity in co-transfected cells was detected using the Dual-Luciferase Reporter Assay System (Promega Corporation) and GloMax® Explorer Multimode Microplate Reader (Promega Corporation). Firefly luciferase activity was used as the main reporter activity, and *Renilla* luciferase activity was used as the control for normalization.

Statistical analysis. Data are presented as the mean ± SEM from at least three repetitions. Unpaired Student's t-test was used to perform statistical analysis of two unpaired groups, while paired Student's t-test was used to perform statistical analysis of two paired groups (Microsoft Excel 2010; Microsoft Corporation). In addition, one-way ANOVA was used to perform statistical analysis of multiple groups (GraphPad Prism 8; GraphPad Software, Inc.). $P<0.05$ was considered to indicate a statistically significant difference.

Results

Identification of LINC01635 as an lncRNA with CT expression pattern. To screen for differentially expressed lncRNAs in lung cancer, the gene expression profile of lung adenocarcinoma and normal lung tissue was obtained from GEO dataset GSE113852, which contained the expression data of 27 lung tumor samples and 27 normal lung samples. With $Log_2FC>2$ as the screen threshold, 168 genes were highly expressed in lung adenocarcinoma compared with those in normal lung tissues (Fig. 1A). The expression of these genes in physiological conditions was assessed by analyzing the HPA RNA-seq normal tissue database, and only LINC01635 (ENSG00000228397; Log2FC=2.36; $P=8.58x10^{-8}$) was found to be highly expressed in the testis (Fig. 1B). LINC01635 was located on chromosome 1p36.12, upstream of human cell division cycle 42 (CDC42) in the human genome, but its transcriptional direction is opposite to that of CDC42. The lncRNA property of LINC01635 was confirmed by evaluating its coding potential (CPAT and CNCI tools) and predicting the secondary structure (Fig. 1B). Furthermore, a high LINC01635 expression level was also confirmed in lung cancer samples by analyzing another GEO dataset using lnCAR online tools (GSE101929; Fig. 1D). In addition, the expression level of LINC01635 was analyzed in multiple cancer types compared with corresponding normal tissues (TCGA and GTEx data), and LINC01635 was highly expressed in multiple cancer types and testis tissues (Fig. 1E). To analyze the common high expression pattern of LINC01635 in different human cancer types, its expression level in all cancer types was compared with that in all normal tissues excluding testis. LINC01635 was found to be significantly upregulated in cancer (Fig. 1E).

To validate the data from the bioinformatics analysis, the expression of LINC01635 was firstly checked in samples from human patients with NSCLC (Table II). All patients were diagnosed with LAD NSCLC according to histopathological evaluation. No radiotherapy or chemotherapy was performed before the surgery or puncture. The ΔCq values ($Cq_{LINC01636}$-Cq_{GAPDH}) in the lung cancer tissues were lower than those in the normal lung tissues, which showed that

Table II. Characteristics of the patient tissue samples.

Characteristic	Value
Mean age ± SD, years	69.00±7.71
Sex, % (n/total n)	
Male	71.4 (10/14)
Female	28.6 (4/14)
Histological classification, % (n/total n)	
Adenocarcinoma	50.0 (7/14)
Squamous	50.0 (7/14)
TNM stage, % (n/total n)	
I	28.6 (4/14)
II	21.4 (3/14)
III	14.3 (2/14)
IV	35.7 (5/14)
Lymph node metastasis, % (n/total n)	
N0	78.6 (11/14)
N1	21.4 (3/14)
N2	0.0 (0/14)
N3	0.0 (0/14)
Tumor location, % (n/total n)	
Left	42.9 (6/14)
Right	57.1 (8/14)

TNM, Tumor-Node-Metastasis (53).

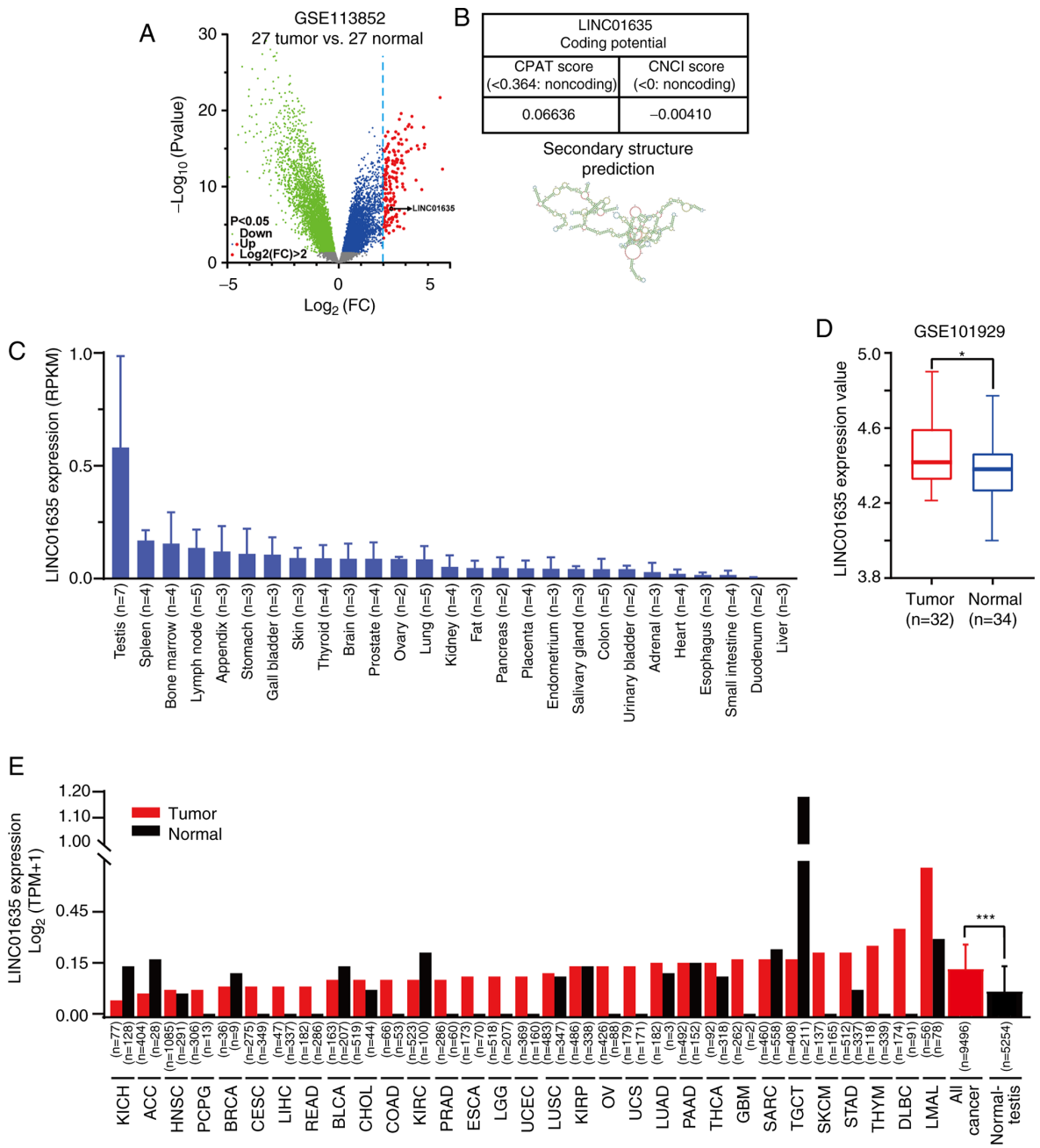

Figure 1. LINC01635 is a long non-coding RNA with a cancer/testis expression pattern. (A) The volcano map of differentially expression genes of the GSE113852 dataset, which contains the expression profiles of 27 lung adenocarcinoma and 27 normal lung tissue samples. The green dots represent downregulated genes (P<0.05), the blue dots represent upregulated genes (P<0.05) and the red dots represent upregulated genes (P<0.05) for which the value of $\log_2$(FC) was >2. The $\log_2$(FC) value of LINC01635 was 2.36, and the P-value was 8.58×10^{-8}. (B) Non-coding property prediction of LINC01635, including CPAT, CNCI and Secondary Structure Prediction tools. (C) Expression in RPKM of LINC01635 among the Human Protein Atlas RNA-seq normal tissue datasets. (D) The overexpression of LINC01635 in lung cancer tissues was confirmed by analyzing GSE101929 datasets using lnCAR online tools. (E) Expression of LINC01635 in tumor and normal tissue samples from GTEx and TCGA database. *P<0.05; ***P<0.001. LINC01635, long intergenic non-protein coding RNA 1635; CPAT, coding-potential assessment tool; CNCI, coding-non-coding index; RPKM, reads per kilobase million; RNA-seq, RNA-sequencing; lnCAR, lncRNAs from cancer arrays; TCGA, The Cancer Genome Atlas; KICH, kidney chromophobe; ACC, adrenocortical carcinoma; HNSC, head and neck squamous cell carcinoma; PCPG, pheochromocytoma and paraganglioma; BRCA, breast invasive carcinoma; CESC, cervical squamous cell carcinoma and endocervical adenocarcinoma; LIHC, liver hepatocellular carcinoma; READ, rectal adenocarcinoma; BLCA, bladder urothelial carcinoma; CHOL, cholangiocarcinoma; COAD, colon adenocarcinoma; KIRC, kidney renal clear cell carcinoma; PRAD, prostate adenocarcinoma; ESCA, esophageal carcinoma; LGG, brain lower grade glioma; UCEC, uterine corpus endometrial carcinoma; LUSC, lung squamous cell carcinoma; KIRP, kidney renal papillary cell carcinoma; OV, ovarian serous cystadenocarcinoma; UCS, uterine carcinosarcoma; LUAD, lung adenocarcinoma; PAAD, pancreatic adenocarcinoma; THCA, thyroid carcinoma; GBM, glioblastoma multiforme; SARC, sarcoma; TGCT, testicular germ cell tumor; SKCM, skin cutaneous melanoma; STAD, stomach adenocarcinoma; THYM, thymoma; DLBC, lymphoid neoplasm diffuse large B-cell lymphoma; LAML, acute myeloid leukemia.

the expression level of LINC01635 was significantly higher in the 14 NSCLC tissues than in the corresponding normal lung tissues (P<0.05; Fig. 2A). Next, the expression level of LINC01635 was examined in four human lung cancer cell lines (A549, H1299, H1975 and PC9), and LINC01635 was found to be overexpressed in the A549, H1299 and H1975 cell

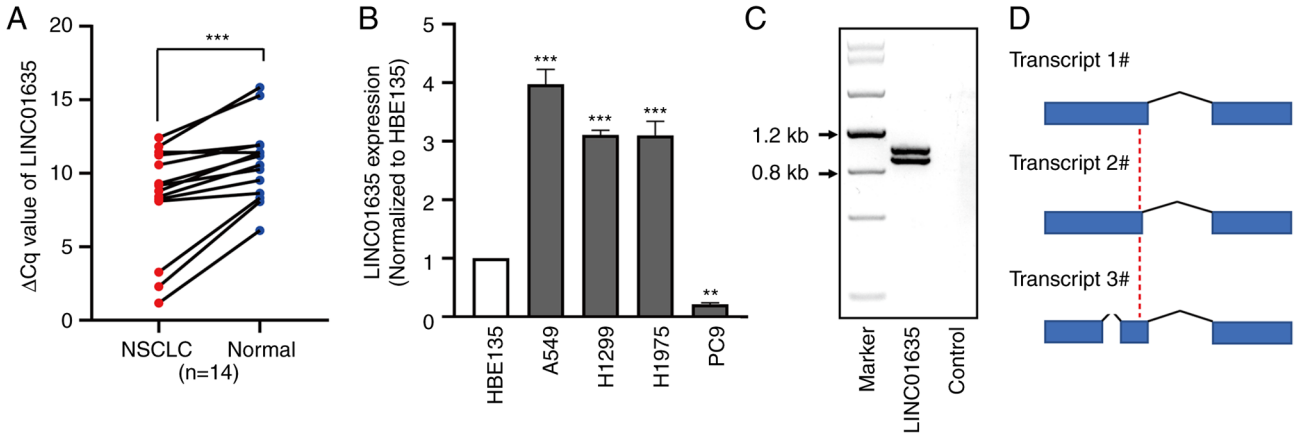

Figure 2. LINC01635 expression is upregulated in NSCLC tissue samples and cell lines. (A) The expression of LINC01635 was significantly increased in NSCLC tissue samples compared with that in adjacent normal lung tissue samples according to RT-qPCR analysis (***P<0.001). (B) The expression of LINC01635 was overexpressed in NSCLC cell lines (A549, H1299 and H1975) compared with that in the normal human bronchial epithelial cell line (HBE135) (**P<0.01 and ***P<0.001 vs. HBE135). (C) Transcripts of LINC01635 were examined by RT-PCR in the A549 cell line, which showed two specific bands. (D) Transcripts of LINC01635 were analyzed according to sequencing reports of all RT-PCR products. Blue boxes represent exons, and polylines represent splicing sites. NSCLC, non-small cell lung cancer; LINC01635, long intergenic non-protein coding RNA 1635; RT-qPCR, reverse transcription-quantitative PCR.

lines by 3.1- to 3.9-fold compared with that in human bronchial epithelial HBE135 cell line, but was reduced to 21% in the PC9 cell line compared with that in the HBE135 cell line (Fig. 2B). Next, according to the prediction of full-length LINC01635 transcript sequences in the Ensembl website, primers were designed to clone LINC01635 in the A549 cell line and two bands of PCR products were found (Fig. 2C). Next, the PCR products were cloned, and the sequencing results showed that LINC01635 in the A549 cell line had three transcripts (Figs. 2D and S1). These results suggested that LINC01635 could be a CT-lncRNA.

Silencing of LINC01635 suppresses the proliferation and migration of lung cancer in cultured cells. To investigate the function of LINC01635 in NSCLC cell lines, LINC01635 was knocked down in A549 and H1975 cell lines by transfection with siRNA, which targeted the common sequence of the three transcripts. After 24 h of transfection, the knockdown efficiency of si-LINC01635 was 70.7% in the A549 cell line and 53.5% in the H1975 cell line, compared with transfection with NC siRNA (Fig. 3A and B). It is worth noting that the designed siRNA also targeted LINC00339, which was partially overlapped but transcriptionally opposite to LINC01635. The expression of LINC00339 was examined in the lung cell lines, as well as the effect of the siRNA on LINC00339. LINC00339 was also highly expressed in the A549 and H1975 cell lines, but the designed siRNA could not efficiently downregulate the expression of LINC00339 in either cell line (Fig. S2). Next, the role of LINC01635 in the proliferation of NSCLC cells was examined using CCK-8 assays. The results indicated that knockdown of LINC01635 decreased the proliferation in the A549 after 72 h post-transfection and in H1975 cell lines after 48 h post-transfection (Fig. 3C and D). Furthermore, Transwell assays were performed and found that knockdown of LINC01635 also significantly suppressed cell migration in both the A549 and H1975 cell lines (Fig. 3E and F). The expression levels of MMP2 and MMP9, migration-related markers, were also assessed and were shown to be downregulated both at the transcriptional and translational levels when LINC01635 was knocked down (Fig. 3G-I). These results demonstrated that LINC01635 plays important roles in the proliferation and migration of NSCLC cell lines.

Silencing of LINC01635 suppresses the proliferation and metastasis of lung cancer cells in zebrafish xenograft models. To verify whether LINC01635 could regulate the progression of lung cancer *in vivo*, zebrafish xenograft models were used to examine proliferation and metastasis simultaneously. The PVS of zebrafish larvae were implanted with A549 or H1975 cells that were transfected with si-LINC01635 and labeled by CM-DiI. At 1 dpi, the zebrafish larvae with a similar tumor size at the PVS and no CM-DiI signal at other sites were selected according to the CM-DiI-positive area (Fig. S3), and then cultured for further analysis. At 4 dpi, the yolk and trunk of the injected zebrafish larvae were imaged to assess the cell proliferation and metastasis, respectively (27,28). Compared with that for NC siRNA transfection, the CM-DiI-positive region was significantly smaller both in the yolk and trunk when LINC01635 was silenced in A549 cells (Fig. 4A-F). Similar results were also obtained in zebrafish xenograft using H1975 cells (Fig. 4G-L). These results demonstrated that LINC01635 regulates the proliferation and metastasis of lung cancer *in vivo*.

LINC01635 can bind with miR-455-5p and regulates the expression of miR-455-5p-targeting tumor-related genes. To explore the functional mechanism of LINC01635, the subcellular location of LINC01635 was first studied and found to be both in the nucleus and cytoplasm (Fig. 5A). As LINC01635 is located both in the nucleus and cytoplasm of lung cancer cells, it might regulate the downstream genes at the transcriptional and/or post-transcriptional levels. To examine whether LINC01635 could function at the post-transcriptional level

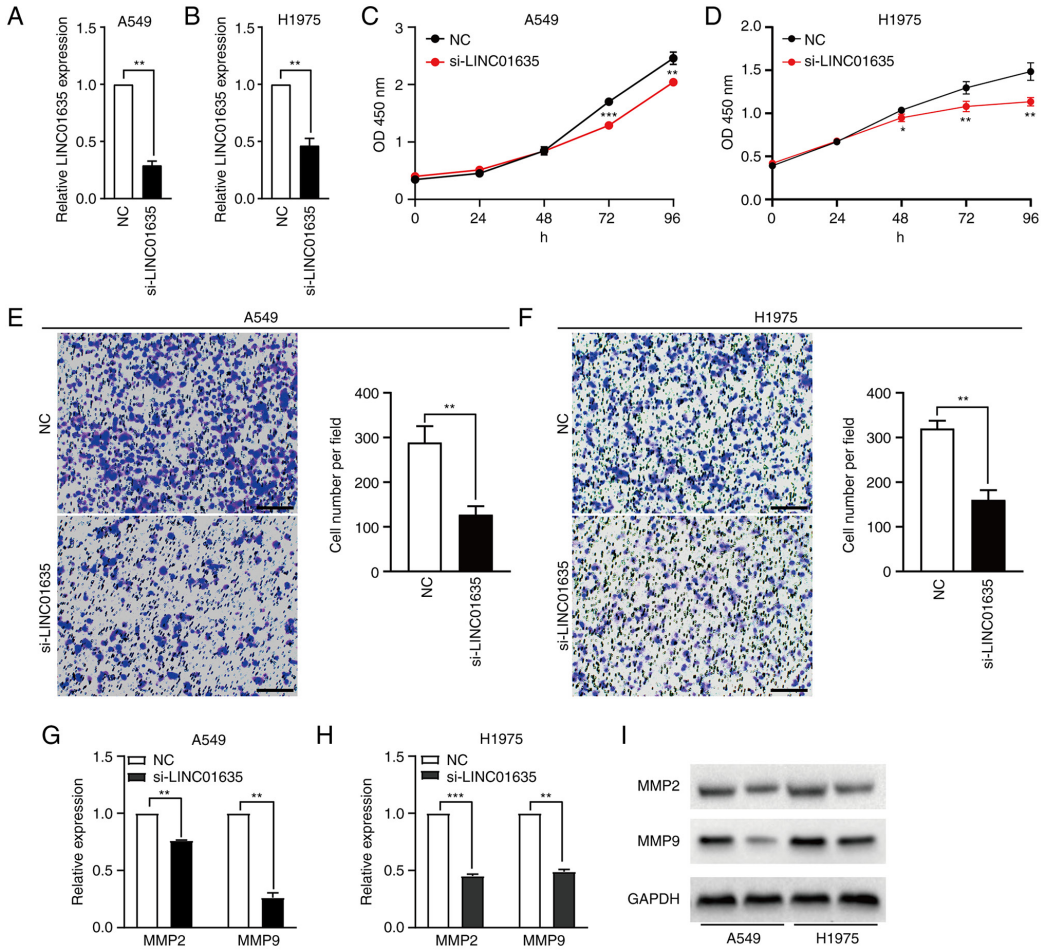

Figure 3. Knockdown of LINC01635 decreases the proliferation and migration in lung cancer cells. (A and B) The knockdown efficiencies of LINC01635 in (A) A549 and (B) H1975 cell lines were examined by reverse transcription-qPCR. (C and D) CCK-8 assays showed that knockdown of LINC01635 decreased the proliferation of (C) A549 and (D) H1975 cells. (E and F) Transwell assays showed knockdown of LINC01635 decreased the migration of (E) A549 and (F) H1975 cells. (G and H) The expression of (G) MMP2 and (H) MMP9 decreased when LINC01635 was knocked down, as assessed by qPCR. (I) The expression of (G) MMP2 and (H) MMP9 decreased when LINC01635 was knocked down, as assessed by western blotting. Scale bar, 100 μm. *P<0.05, **P<0.01, ***P<0.001. qPCR, quantitative PCR; si, small interfering; NC, negative control; LINC01635, long intergenic non-protein coding RNA 1635.

by binding miRNAs, its miRNA binging sites were predicted by miRDB (http://mirdb.org/) (29) and LncBase (30), with 9 microRNA binding sites predicted by both softwares in total. Among these miRNAs, miR-455-5p could bind with all of the transcripts of LINC01635 with highest potential (rank 1; Fig. 5B) (31). To confirm the binding possibility between LINC01635 and miR-455-5p, dual-luciferase reporter plasmids were constructed that contained the wild-type or mutant binding site of LINC01635 (Fig. 5C). The dual-luciferase assay revealed that overexpression of miR-455-5p reduced the luciferase activity of the reporter plasmid containing the LINC01635 sequence, but not that of the reporter plasmid containing the LINC01635 mutant sequence (Fig. 5D). To confirm whether the LINC01635 could regulate a series of tumor-related genes through miR-455-5p, several miR-455-5p-targeting genes (CPEB1, TMED2, HDAC4, STK24, CDKN1B, UBE2V1, USP3, RAB18 and SOX11) that are involved in multiple cancer types were examined (32-40). The majority of these genes were downregulated when knocking down LINC01635 in lung cancer cells, and similar regulation was also observed when overexpressing miR-455-5p (Fig. 5E). These results imply that LINC01635 could regulate the expression of tumor-related genes by targeting miR-455-5p.

Knockdown of miR-455-5p partially rescues the proliferation and migration of lung cancer cells, which is suppressed by LINC01635 silencing. To study the roles of miR-455-5p in lung cancer cells, the expression of miR-455-5p was first downregulated by transfection with the miR-455-5p inhibitor (Fig. 6A). After transfection, the results of CCK-8 and Transwell assays showed that miR-455-5p inhibition promoted the proliferation and migration of the A549 cells (Fig. 6B and C). To examine whether miR-455-5p mediates the roles of LINC01635 in the progression of lung cancer cells, si-LINC01635 and miR-455-5p inhibitor were cotransfected into A549 cells simultaneously. The knockdown of LINC01635 suppressed the growth and migration of lung cancer cells, but miR-455-5p inhibitor transfection partially counteracted the suppressive effects of LINC01635 knockdown both in terms of the proliferation and migration of the lung cancer cells (Fig. 6D and E). These results indicate that LINC01635 could promote the progression of lung cancer cells via the miR-455-5p-mediated pathway.

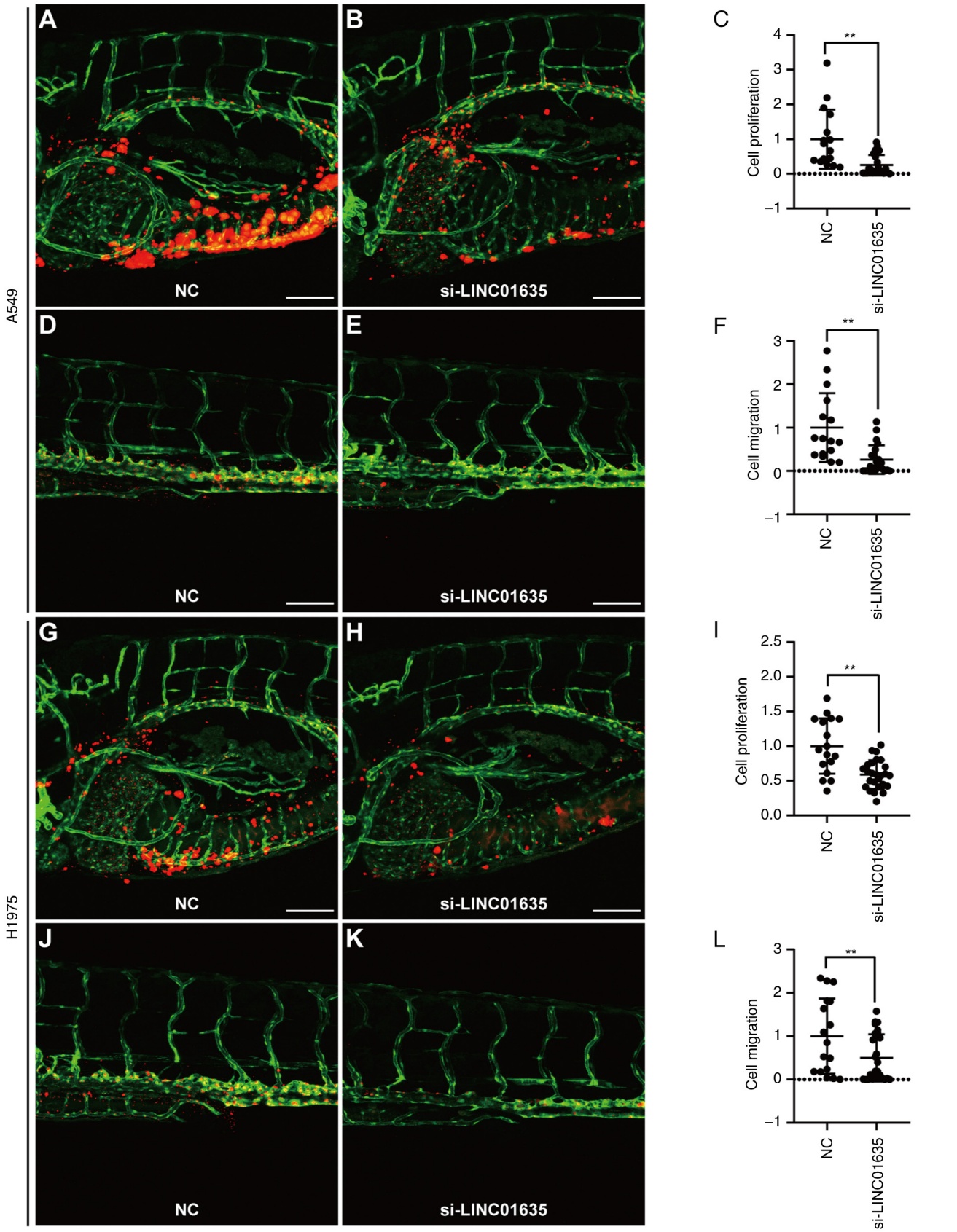

Figure 4. Knockdown of LINC01635 decreases the proliferation and metastasis of lung cancer cells in a zebrafish xenograft. (A-F) Zebrafish xenograft models showed that knockdown of LINC01635 decreased the proliferation and metastasis of A549 cells at 4 dpi. A549 cells transfected with (A and D) NC and (B and E) si-LINC01635 were labeled with CM-DiI and then injected into the PVS of 2-days post-fertilization Tg(fli1a:EGFP) transgenic zebrafish larvae, which labeled the zebrafish endothelial cells. Confocal images were taken at 4 dpi. (A and B) The tumor cells in the PVS were quantified for cell proliferation, (D and E) and the tumor cells in the trunk were quantified for cell metastasis. Statistical analysis of (C) proliferation and (F) metastasis when knocking down LINC01635 in A549 cells compared with the NC. (G-L) Zebrafish xenograft models showed that knockdown of LINC01635 decreased the proliferation and metastasis of H1975 cells. Scale bar, 100 μm. **P<0.01. dpi, days post-injection; si, small interfering; NC, negative control; LINC01635, long intergenic non-protein coding RNA 1635; PVS, perivitelline space.

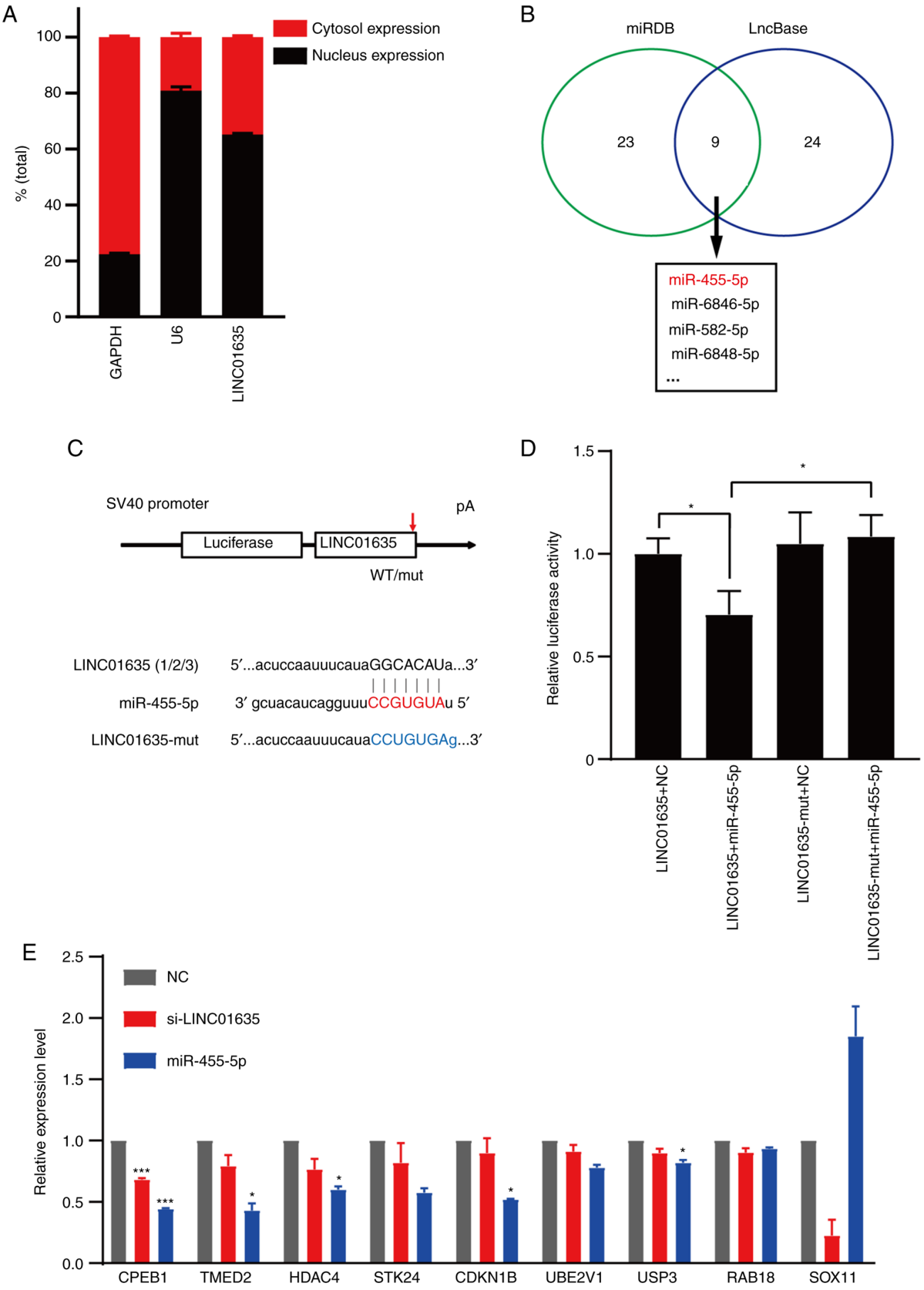

Figure 5. LINC01635 can bind with miR-455-5p and regulate the expression of miR-455-5p-targeting tumor-related genes. (A) LINC01635 subcellular location in A549 was assessed by RT-qPCR after nuclear and cytosolic separation of total RNA. GAPDH was used as a cytosol marker and U6 was used as a nucleus marker. (B) miRNA binding sites of LINC01635 were predicted by miRDB and LncBase tools; 9 miRNAs were predicted by both tools and miR-455-5p had the highest potential for binding with LINC01635. (C) Binding site between LINC01635 transcripts and miR-455-5p, and the LINC01635 with the binding site mutant (LINC01635-mut). The red arrow represents the site of the miR-455-5p targeting site. (D) Dual-luciferase reporter assay showed that LINC01635 could bind with miR-455-5p directly. The relative luciferase reporter activity was reduced when co-transfecting with miR-455-5p mimic and LINC01635 reporter plasmid, but not LINC01635-mut reporter plasmid (*P<0.05). (E) The expression level of miR-455-5p-targeting tumor-related genes was examined by RT-qPCR following knockdown of LINC01635 or overexpression of miR-455-5p (*P<0.05 and ***P<0.001 vs. NC). miR/miRNA, microRNA; si, small interfering; NC, negative control; LINC01635, long intergenic non-protein coding RNA 1635; RT-qPCR, reverse transcription-quantitative PCR; WT, wild-type; mut, mutant.

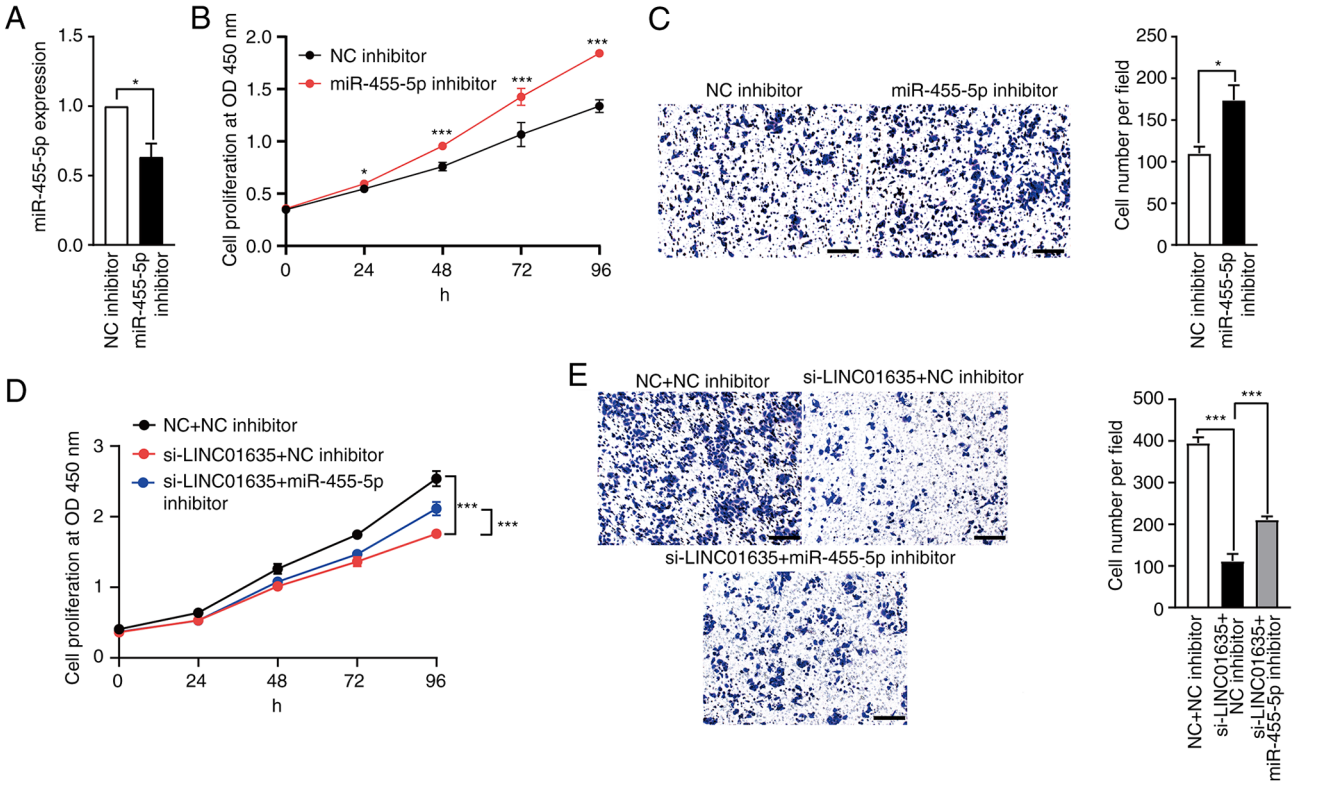

Figure 6. Knockdown of miR-455-5p partially rescues the proliferation and migration of lung cancer cells, which is suppressed by LINC01635 silencing. (A) The knockdown efficiencies of miR-455-5p in A549 cell lines were examined by reverse transcription-quantitative PCR (*P<0.05). (B) CCK-8 assays showed that knockdown of miR-455-5p increased the proliferation of A549 cells (*P<0.05 and ***P<0.001 vs. NC inhibitor). (C) Transwell assays showed that knockdown of miR-455-5p increased the migration of A549 cells (*P<0.05). (D) CCK-8 assays showed that knockdown of miR-455-5p partially rescued the proliferation of A549 cells, which was suppressed by LINC01635 silencing (***P<0.001). (E) Transwell assays showed that knockdown of miR-455-5p partially rescued the migration of A549 cells, which was suppressed by LINC01635 silencing (***P<0.001). Scale bar, 100 μm. miR/miRNA, microRNA; si, small interfering; NC, negative control; LINC01635, long intergenic non-protein coding RNA 1635.

Discussion

An increasing number of studies have reported that lncRNAs play important roles in the development and progression of NSCLC through different signal pathways (13,41-43). The present study found that LINC01635 was upregulated in lung cancer tissues and cell lines. Functional experiments showed that LINC01635 promoted the proliferation and metastasis of NSCLC cells *in vitro* and *in vivo*. Moreover, LINC01635 was able to bind miR-455-5p and regulated the expression of a series of miR-455-5p-targeting tumor-related genes. These findings suggest that LINC01635 could regulate NSCLC progression though binding with miR-455-5p.

CT genes are a diverse group of genes that are restrictively expressed in the testis under normal conditions, but they are also expressed in ~40% of different types of cancer (44). Similar to tumors, the testes exhibit abundant cell division, migration and immortalization (45), and lots of testicular genes are considered as promising cancer biomarkers and treatment targets (14). Moreover, the similarities in cellular processes between gametogenesis and tumorigenesis also provide valuable insights into understanding the mechanism of tumorigenesis. CT-lncRNA represents a new direction for the study of lncRNA mechanisms in tumor biology. For example, Hosono *et al* (16) demonstrated that THOR is a conserved CT-lncRNA and that it promotes the progression of lung cancer through interaction with IGF2BP1 (16). Tan *et al* (19) showed that CT-lncRNA PACT6 facilitates the malignant phenotype of ovarian cancer through binding with miR-143-3p (19). In the present study, by screening the GEO database of lung cancer tissues and the HPA RNA-seq normal tissue database, LINC01635 was revealed to be a novel CT-lncRNA that promotes lung cancer progression by binding with miR-455-5p. However, in the present study, mainly the basic cellular functions of LINC01635 in lung cancer cells were assessed through the examination of the migration and invasion biomarkers MMP2 and MMP9 in cultured cell lines, and the detailed molecular mechanism of LINC01635 shall be analyzed by examining different biomarkers in future studies.

It has been reported that lncRNAs play important roles in proliferation, differentiation, metastasis, metabolism and apoptosis in cancer progression by regulating their target genes at the transcriptional, post-transcriptional and epigenetic levels (7,8). Different regulatory functions depend on the subcellular locations and interactions with specific molecules (46). In the nucleus, lncRNAs generally function by modulating transcriptional programs through chromatin interactions and remodeling by formatting the scaffolding complex (47,48). In the cytoplasm, lncRNAs function by regulating translational and/or post-transcriptional programs to affect gene expression levels. In addition, numerous lncRNAs have been identified as competing endogenous RNAs (ceRNAs) that can regulate the expression of target genes at the post-transcriptional level by competitive binding with miRNAs in the cytoplasm (49). The

present study found LINC01635 located in both the nucleus and cytoplasm, which implies that LINC01635 may play regulatory roles at both the transcriptional and post-transcriptional levels. To examine whether LINC01635 could function as a ceRNA, the binding sites of miRNAs in LINC01635 were predicted by cross-comparison analysis between the miRDB and LncBase database, and miR-455-5p was screened out with the highest potential. Furthermore, the present data not only demonstrated that miR-455-5p could bind with LINC01635 directly *in vitro*, but also showed that miR-455-5p inhibition could partially rescue the suppression effects caused by LINC01635 knockdown, which implies that LINC01635/miR-455-5p may function as a ceRNA network.

The present study also examined the expression of a series of miR-455-5p-targeting tumor-related genes following the knockdown of LINC01635 or the overexpression of miR-455-5p, and found that the changes in the expression of some genes was associated. These genes may regulate tumor progression through different pathways. CDKN1B can shift from cyclin-dependent kinase inhibitor to oncogene by regulating the cell cycle in a cyclin-dependent kinase-dependent or -independent manner (36,50). SOX11, a transcription factor, mainly regulates progenitor and stem cell behavior during embryogenesis, and it also expressed in a wide variety of cancer types, such as neck cancer, malignant glioma, ovarian cancer and breast cancer (40,51). RAB18 is a member of the Ras oncogene superfamily, which promotes cell invasion and inhibits cell apoptosis in various cancer types, such as hepatocellular carcinoma and gastric cancer (39,52). UBE2V1 is a member of the ubiquitin-conjugating E2 enzyme variant proteins, and it has been reported as an oncogene that acts via ubiquitination and degradation of SIRT1 (37). USP3 is a deubiquitinase that accelerates tumor proliferation and epithelial-to-mesenchymal transition (EMT) via deubiquitinating KLF5 (38). According to the association in expression between LINC01635 and these genes, our future studies shall focus on CPEB1, TMED2 and HDAC4, which might reveal the novel mechanism of LINC01635/miR-455-5p regulatory pathways.

Zebrafish xenografts have been demonstrated as effective models for tumor research (25,26). Compared with mouse models, zebrafish xenografts have obvious advantages. First, the zebrafish xenograft model offers a fast *in vivo* evaluation method of tumor proliferation and metastasis by using same group of transplanted zebrafish larvae. When using mouse xenograft models, it requires two separate models for evaluating the proliferation and metastasis of the tumor cells, respectively. Second, with the help of transparent larvae, the zebrafish xenograft model supplies intuitive studies at the cellular level. The zebrafish xenograft model can be used to assess proliferation and metastasis in only 1 week by transiently transfecting siRNAs, instead of 2-4 weeks in mouse xenograft models, which have to construct stable cell lines using shRNA plasmids. Third, by combining different types of transgenic lines that label different cell types, zebrafish xenograft can be used for studying the tumor microenvironment *in vivo*, including angiogenesis and immune reactions. In mouse xenograft models, it usually requires additional staining steps for the quantification *in vitro*. The results of the zebrafish xenograft model experiments in the present study showed that the silencing of LINC01635 decreased the proliferation and metastasis of the NSCLC cells, which was consistent with the data from the cultured cells, suggesting that a zebrafish xenograft is a good alternative *in vivo* model for examining tumor biology.

In summary, the present study demonstrated LINC01635 is a novel CT-lncRNA and that it promotes the proliferation and metastasis of lung cancer by regulating miR-455-5p-targeting tumor-related genes. These findings indicate that LINC01635 could be a potential biomarker and treatment target for lung cancer.

Acknowledgements

Not applicable.

Funding

The present study was supported by the Research Fund of Lianshui County People's Hospital (2020), and The Program of Innovation and Entrepreneurship Doctor of Jiangsu Province (2021).

Availability of data and materials

The datasets used and/or analyzed during the current study are available from the corresponding author on reasonable request. Microarray datasets GSE113852 (20) and GSE101929 (21) were downloaded from the Gene Expression Omnibus database.

Authors' contributions

YZ conceived and designed the study. WS, JP, SG, JS, LW, BT and JC acquired the data. JS, LW, BT and JC collected the patient samples. SG, JS and LW created the zebrafish xenograft model. BT and JC performed the reverse transcription-quantitative PCR experiments. WS and JP performed the rest of the experiments, and analyzed and interpreted the data. SG performed the statistical analysis and wrote the manuscript. WS, JP and YZ revised the manuscript. WS, JP, SG, JS, LW, BT, JC and YZ confirm the authenticity of all the raw data. All authors read and approved the final version of the manuscript.

Ethics approval and consent to participate

All animal experiments were approved by the Institutional Animal Care and Use Committee of The Lianshui County People's Hospital, Kangda College of Nanjing Medical University (Huai'an, China). All patients enrolled in this study were informed of the study details and provided written informed consent. The use of the clinical samples was approved by The Medical Ethics Committee of Lianshui County People's Hospital, Kangda College of Nanjing Medical University.

Patient consent for publication

Not applicable.

Competing interests

The authors declare that they have no competing interests.

References

1. Bade BC and Dela Cruz CS: Lung cancer 2020: Epidemiology, etiology, and prevention. Clin Chest Med 41: 1-24, 2020.
2. Venkatesan P: IASLC 2020 world conference on lung cancer. Lancet Respir Med 8: e76, 2020.
3. Herbst RS, Morgensztern D and Boshoff C: The biology and management of non-small cell lung cancer. Nature 553: 446-454, 2018.
4. Molina JR, Yang P, Cassivi SD, Schild SE and Adjei AA: Non-small cell lung cancer: Epidemiology, risk factors, treatment, and survivorship. Mayo Clin Proc 83: 584-594, 2008.
5. Hirsch FR, Scagliotti GV, Mulshine JL, Kwon R, Curran WJ Jr, Wu YL and Paz-Ares L: Lung cancer: Current therapies and new targeted treatments. Lancet 389: 299-311, 2017.
6. Carninci P, Kasukawa T, Katayama S, Gough J, Frith MC, Maeda N, Oyama R, Ravasi T, Lenhard B, Wells C, *et al*: The transcriptional landscape of the mammalian genome. Science 309: 1559-1563, 2005.
7. Nagano T and Fraser P: No-nonsense functions for long noncoding RNAs. Cell 145: 178-181, 2011.
8. Sanchez Calle A, Kawamura Y, Yamamoto Y, Takeshita F and Ochiya T: Emerging roles of long non-coding RNA in cancer. Cancer Sci 109: 2093-2100, 2018.
9. Wang L, Chen Z, An L, Wang Y, Zhang Z, Guo Y and Liu C: Analysis of long non-coding RNA expression profiles in non-small cell lung cancer. Cell Physiol Biochem 38: 2389-2400, 2016.
10. Qiu M, Feng D, Zhang H, Xia W, Xu Y, Wang J, Dong G, Zhang Y, Yin R and Xu L: Comprehensive analysis of lncRNA expression profiles and identification of functional lncRNAs in lung adenocarcinoma. Oncotarget 7: 16012-16022, 2016.
11. Chen J, Wang R, Zhang K and Chen LB: Long non-coding RNAs in non-small cell lung cancer as biomarkers and therapeutic targets. J Cell Mol Med 18: 2425-2436, 2014.
12. Xu YJ, Du Y and Fan Y: Long noncoding RNAs in lung cancer: What we know in 2015. Clin Transl Oncol 18: 660-665, 2016.
13. Chen Z, Lei T, Chen X, Gu J, Huang J, Lu B and Wang Z: Long non-coding RNA in lung cancer. Clin Chim Acta 504: 190-200, 2020.
14. Whitehurst AW: Cause and consequence of cancer/testis antigen activation in cancer. Annu Rev Pharmacol Toxicol 54: 251-272, 2014.
15. Babatunde KA, Najafi A, Salehipour P, Modarressi MH and Mobasheri MB: Cancer/testis genes in relation to sperm biology and function. Iran J Basic Med Sci 20: 967-974, 2017.
16. Hosono Y, Niknafs YS, Prensner JR, Iyer MK, Dhanasekaran SM, Mehra R, Pitchiaya S, Tien J, Escara-Wilke J, Poliakov A, *et al*: Oncogenic role of THOR, a conserved cancer/testis long non-coding RNA. Cell 171: 1559-1572 e20, 2017.
17. Qin N, Wang C, Lu Q, Ma Z, Dai J, Ma H, Jin G, Shen H and Hu Z: Systematic identification of long non-coding RNAs with cancer-testis expression patterns in 14 cancer types. Oncotarget 8: 94769-94779, 2017.
18. Chen S, Chen Y, Qian Q, Wang X, Chang Y, Ju S, Xu Y, Zhang C, Qin N, Ding H, *et al*: Gene amplification derived a cancer-testis long noncoding RNA PCAT6 regulates cell proliferation and migration in hepatocellular carcinoma. Cancer Med 8: 3017-3025, 2019.
19. Tan X, Shao Y, Teng Y, Liu S, Li W, Xue L, Cao Y, Sun C, Zhang J, Han J, *et al*: The cancer-testis long non-coding RNA PCAT6 facilitates the malignant phenotype of ovarian cancer by sponging miR-143-3p. Front Cell Dev Biol 9: 593677, 2021.
20. Roth A, Boulay K, Groß M, Polycarpou-Schwarz M, Mallette FA, Regnier M, Bida O, Ginsberg D, Warth A, Schnabel PA, *et al*: Targeting LINC00673 expression triggers cellular senescence in lung cancer. RNA Biol 15: 1499-1511, 2018.
21. Mitchell KA, Zingone A, Toulabi L, Boeckelman J and Ryan BM: Comparative transcriptome profiling reveals coding and noncoding RNA differences in NSCLC from African Americans and European Americans. Clin Cancer Res 23: 7412-7425, 2017.
22. Zheng Y, Xu Q, Liu M, Hu H, Xie Y, Zuo Z and Ren J: lnCAR: A comprehensive resource for lncRNAs from cancer arrays. Cancer Res 79: 2076-2083, 2019.
23. Tang Z, Li C, Kang B, Gao G, Li C and Zhang Z: GEPIA: A web server for cancer and normal gene expression profiling and interactive analyses. Nucleic Acids Res 45: W98-W102, 2017.
24. Czimmerer Z, Hulvely J, Simandi Z, Varallyay E, Havelda Z, Szabo E, Varga A, Dezso B, Balogh M, Horvath A, *et al*: A versatile method to design stem-loop primer-based quantitative PCR assays for detecting small regulatory RNA molecules. PLoS One 8: e55168, 2013.
25. Hu R, Fan C, Li H, Zhang Q and Fu YF: Evaluation of putative reference genes for gene expression normalization in soybean by quantitative real-time RT-PCR. BMC Mol Biol 10: 93, 2009.
26. Lawson ND and Weinstein BM: In vivo imaging of embryonic vascular development using transgenic zebrafish. Dev Biol 248: 307-318, 2002.
27. Fior R, Póvoa V, Mendes RV, Carvalho T, Gomes A, Figueiredo N and Ferreira MG: Single-cell functional and chemosensitive profiling of combinatorial colorectal therapy in zebrafish xenografts. Proc Natl Acad Sci USA 114: E8234-E8243, 2017.
28. Hason M and Bartůněk P: Zebrafish models of cancer-new insights on modeling human cancer in a non-mammalian vertebrate. Genes (Basel) 10: 935, 2019.
29. Chen Y and Wang X: miRDB: An online database for prediction of functional microRNA targets. Nucleic Acids Res 48: D127-D131, 2020.
30. Paraskevopoulou MD, Vlachos IS, Karagkouni D, Georgakilas G, Kanellos I, Vergoulis T, Zagganas K, Tsanakas P, Floros E, Dalamagas T, *et al*: DIANA-LncBase v2: Indexing microRNA targets on non-coding transcripts. Nucleic Acids Res 44: D231-D238, 2016.
31. Xing Q, Xie H, Zhu B, Sun Z and Huang Y: MiR-455-5p suppresses the progression of prostate cancer by targeting CCR5. Biomed Res Int 2019: 6394784, 2019.
32. Xu M, Fang S, Song J, Chen M, Zhang Q, Weng Q, Fan X, Chen W, Wu X, Wu F, *et al*: CPEB1 mediates hepatocellular carcinoma cancer stemness and chemoresistance. Cell Death Dis 9: 957, 2018.
33. Shi-Peng G, Chun-Lin C, Huan W, Fan-Liang M, Yong-Ning C, Ya-Di Z, Guang-Ping Z and Ye-Ping C: TMED2 promotes epithelial ovarian cancer growth. Oncotarget 8: 94151-94165, 2017.
34. Jin K, Zhao W, Xie X, Pan Y, Wang K and Zhang H: MiR-520b restrains cell growth by targeting HDAC4 in lung cancer. Thorac Cancer 9: 1249-1254, 2018.
35. Huang N, Lin W, Shi X and Tao T: STK24 expression is modulated by DNA copy number/methylation in lung adenocarcinoma and predicts poor survival. Future Oncol 14: 2253-2263, 2018.
36. Belletti B and Baldassarre G: Roles of CDKN1B in cancer? Aging (Albany NY) 7: 529-530, 2015.
37. Shen T, Cai LD, Liu YH, Li S, Gan WJ, Li XM, Wang JR, Guo PD, Zhou Q, Lu XX, *et al*: Ube2v1-mediated ubiquitination and degradation of Sirt1 promotes metastasis of colorectal cancer by epigenetically suppressing autophagy. J Hematol Oncol 11: 95, 2018.
38. Wu Y, Qin J, Li F, Yang C, Li Z, Zhou Z, Zhang H, Li Y, Wang X, Liu R, *et al*: USP3 promotes breast cancer cell proliferation by deubiquitinating KLF5. J Biol Chem 294: 17837-17847, 2019.
39. Gong T, Zhou B, Liu M, Chen X, Huang S, Xu Y, Luo R and Chen Z: RAB18 promotes proliferation and metastasis in hepatocellular carcinoma. Am J Transl Res 11: 1009-1019, 2019.
40. Huang J, Ji EH, Zhao X, Cui L, Misuno K, Guo M, Huang Z, Chen X and Hu S: Sox11 promotes head and neck cancer progression via the regulation of SDCCAG8. J Exp Clin Cancer Res 38: 138, 2019.
41. Liu XH, Liu ZL, Sun M, Liu J, Wang ZX and De W: The long non-coding RNA HOTAIR indicates a poor prognosis and promotes metastasis in non-small cell lung cancer. BMC Cancer 13: 464, 2013.
42. Tang Y, Xiao G, Chen Y and Deng Y: LncRNA MALAT1 promotes migration and invasion of non-small-cell lung cancer by targeting miR-206 and activating Akt/mTOR signaling. Anticancer Drugs 29: 725-735, 2018.
43. Nie FQ, Sun M, Yang JS, Xie M, Xu TP, Xia R, Liu YW, Liu XH, Zhang EB, Lu KH and Shu YQ: Long noncoding RNA ANRIL promotes non-small cell lung cancer cell proliferation and inhibits apoptosis by silencing KLF2 and P21 expression. Mol Cancer Ther 14: 268-277, 2015.
44. Scanlan MJ, Simpson AJ and Old LJ: The cancer/testis genes: Review, standardization, and commentary. Cancer Immun 4: 1, 2004.
45. Gordeeva O: Cancer-testis antigens: Unique cancer stem cell biomarkers and targets for cancer therapy. Semin Cancer Biol 53: 75-89, 2018.
46. Bridges MC, Daulagala AC and Kourtidis A: LNCcation: lncRNA localization and function. J Cell Biol 220: e202009045, 2021.

47. Melé M and Rinn JL: 'Cat's Cradling' the 3D genome by the Act of LncRNA transcription. Mol Cell 62: 657-664, 2016.
48. Clemson CM, Hutchinson JN, Sara SA, Ensminger AW, Fox AH, Chess A and Lawrence JB: An architectural role for a nuclear noncoding RNA: NEAT1 RNA is essential for the structure of paraspeckles. Mol Cell 33: 717-726, 2009.
49. Qi X, Zhang DH, Wu N, Xiao JH, Wang X and Ma W: ceRNA in cancer: Possible functions and clinical implications. J Med Genet 52: 710-718, 2015.
50. Razavipour SF, Harikumar KB and Slingerland JM: p27 as a transcriptional regulator: New roles in development and cancer. Cancer Res 80: 3451-3458, 2020.
51. Tsang SM, Oliemuller E and Howard BA: Regulatory roles for SOX11 in development, stem cells and cancer. Semin Cancer Biol 67: 3-11, 2020.
52. Liu J, Zhang J, Li Y, Wang L, Sui B and Dai D: MiR-455-5p acts as a novel tumor suppressor in gastric cancer by down-regulating RAB18. Gene 592: 308-315, 2016.
53. Lim W, Ridge CA, Nicholson AG and Mirsadraee S: The 8 th lung cancer TNM classification and clinical staging system: review of the changes and clinical implications. Quant Imaging Med Surg 8: 709-718, 2018.